Journal of Applied Polymer Science

Mechanical behavior at nanoscale of chitosan-coated PE surface

Elena Stoleru (Paslaru),[1] Yuliy Tsekov,[2] Rumiana Kotsilkova,[2] Evgeni Ivanov,[2] Cornelia Vasile[1]

[1]"Petru Poni" Institute of Macromolecular Chemistry, Physical Chemistry Department, 41A Gr. Ghica Voda Alley, 700487, Iasi, Romania

[2]Bulgarian Academy of Sciences, Institute of Mechanics, Open Laboratory for Experimental Micro and Nano Mechanics, Acad. G. Bonchev Street, Block 4, 1113 Sofia, Bulgaria

Correspondence to: C. Vasile (E-mail: cvasile@icmpp.ro)

ABSTRACT: Chitosan coating of polyethylene (PE) was proposed as a new procedure to improve its biocompatibility and surface properties. The functionalization of the PE film surface by covalent bonding of chitosan coating and its effect on the surface mechanical properties, as surface elasticity, stiffness, and adhesion (that are important in different biological processes) were investigated by nano-indentation, scratch, and atomic force microscopy. It has been established that chitosan grafting onto corona functionalized PE surface using various coupling agents significantly improves the surface hardness and elastic modulus although they decrease in depth of the layer. Compared to the neat PE substrate, the chitosan coated samples show significant improved friction properties and tear resistance. The surface roughness features correlate with the micro-mechanical parameters. Therefore, the covalent immobilization of the chitosan onto PE leads to a stable coating with better mechanical performance being recommended as a promising material for medical applications and food packaging. © 2015 Wiley Periodicals, Inc. J. Appl. Polym. Sci. **2015**, *132*, 42344.

KEYWORDS: coatings; polyolefins; surfaces and interfaces

Received 29 December 2014; accepted 11 April 2015
DOI: 10.1002/app.42344

INTRODUCTION

Polyethylene (PE) was widely used in various applications because of its excellent mechanical (high specific modulus and strength), chemical resistance, and good thermal properties.[1] However, because of its smooth and nonpolar surface, the adhesion to other materials is poor and its biocompatibility is insufficient. Although PE presents high barrier resistance against water vapor it has relatively high oxygen permeability, which represents a drawback in food packaging applications. Chitosan coating of PE could represent a good procedure for obtaining new materials with decreased gas permeability and, additionally with antibacterial properties.[2] Moreover, chitosan is a biopolymer, which can improve the biocompatibility of the PE. Gas permeability of carbohydrate films and coatings depends on several factors such as film integrity, crystallinity, hydrophilic–hydrophobic ratio, and polymeric chain mobility, interaction between the film-forming polymer and plasticizer or other additives. The surface topography and presence of polar groups on the surface play a crucial role to obtain good adhesion, as adhesion occurs either through physical or chemical interactions as well as mechanical interlocking between the surface and adhesive (coating).[3] Therefore, the design and the optimization of the coating composition are very important for food packaging materials.[4]

Various approaches,[5] such as plasma,[1,6,7] γ-ray irradiation,[8,9] photochemical,[10] ozone treatment,[11] and so on, have been applied for the surface modification of hydrophobic polymers. Corona discharge in air or followed by air exposure oxidizes the film surface, implementing onto this various oxygen and nitrogen-containing functional groups.[12] Shin *et al.*[13] used plasma source ion implantation technique to improve the adhesion between linear low-density PE (LDPE) and chitosan or corn zein protein. Chitosan was immobilized onto low-temperature plasma-treated LDPE surface via polyacrylic acid (PAA) brushes grafted on the polymer surface[14] or onto PE surface treated by dielectric barrier discharge (DBD) under medium vacuum pressure in the presence of air gas.[15]

In our previous study[16] the corona-discharge treatment was used to induce physical–chemical surface modifications to PE, mainly by the implantation of oxygen containing groups, thus a favorable surface environment for chitosan adsorption/grafting has been created. The formation of new oxygen-containing functionalities after corona treatment and amine and amide groups after chitosan coating/grafting were detected and analyzed by Attenuated Total Reflectance-Fourier Transform Infrared Spectroscopy (ATR–FTIR) and X-ray Photoelectron Spectroscopy (XPS). It was established that chitosan was

attached only to the corona-treated PE (PEc) surface and not on the native polymer.

Following the studies carried out by other authors[14,15] and our previous researches[16] it can conclude that simply corona or DBD treatment of PE are not enough to link a chitosan layer stable over time. With this purpose, a two-step procedure consisting in corona discharge treatment coupled with chemical activation using coupling agents [1-ethyl-3-[3-dimethylaminopropyl]carbodiimide hydrochloride/N-hydroxysuccinimide (EDC/NHS) and carbonyldiimidazole (CDI)] was proposed which could lead to covalent bonding of chitosan on PE surface mainly by the formation of amide groups and other types of linkages, and thus a stable surface layer of chitosan resulted. As far as we know, the direct coupling of chitosan by the functional groups implanted onto the PE surface after corona treatment and air exposure, through coupling routes, were not used until now.

The adhesion of a polymer to solid substrates is influenced by their interfacial interaction (physically or chemically), the loss function (dissipation energy) of polymer, and loading angle. Application of suitable coupling agent improves the interfacial bonding and overall adhesion.[17] There are different studies that have shown significant differences in the local interfacial Young's modulus and hardness between the polymer-treated composites and the uncoupled control specimens.[18]

Conventional characterization techniques are not appropriate to measure of mechanical and adhesion properties of thin functional layers on substrate. Nano-indentation and nanoscratch testing are alternative approaching methods. Both techniques have become important tools for probing the mechanical properties at the nanoscale materials.[19]

The surface mechanical properties as surface elasticity, stiffness, and adhesion play a central role in a large number of biological processes being of significant importance for biomedical applications. The ability to measure properties on the nanometer length scale is particularly important for characterization of the surface properties in which the localized material structure has a significant impact on the overall behavior. Nano-indentation is a promising method of measuring the mechanical properties of materials at smaller length and load scales than allowed by other testing methods, thus allowing individual constituents and local regions of heterogeneous materials to be characterized individually.[20]

Atomic force microscopy (AFM) is one of the foremost tools for imaging and measuring surface roughness and topography at the nanoscale, and for the characterization of interface region.[21]

In spite that the chitosan-modified PE film represents a promising material for biomedical/food packaging applications, to our best knowledge the effect of chitosan deposition on the mechanical properties of PE surface was not studied until now in the referred literature. To fill the gap, the objective of this study was to improve surface mechanical properties of PE film by grafting chitosan coating and to evaluate how the surface mechanical properties influence the films oxygen permeability. The ability of nano-indentation, scratch, and AFM testing was explored to determine mechanical properties of the chitosan coating at micro and nanoscale. The multiple depth sensing indentation experiments were carried out in order to investigate the mechanical characteristics in depth of the chitosan layer, grafted on neat PE films. Micro-scratch test with increasing normal and tangential loads was applied to determine the tear resistance and friction properties of the coated film. Surface roughness of the coating was visualized and measured by AFM, and further correlated with the micro-mechanical parameters. The obtained results were analyzed to get a deep inside into mechanical performance of the chitosan-coated PE film useful for biomedical/food packaging applications.

EXPERIMENTAL

Materials

PE, with a 0.02 mm thickness, purchased from SC LORACOM SRL (Roman, Romania) was used. Medium molecular weight chitosan (CHT) with 200–800 cP viscosity in 1% acetic acid and 75–85% deacetylation degree from Sigma-Aldrich—Germany was chosen for surface modification of PE. Water-soluble carbodiimide cross-linkers for zero-length, carboxyl-to-amine conjugation, 1-Ethyl-3-[3-dimethylaminopropyl]carbodiimide hydrochloride and N-hydroxysuccinimide, both with purity > 98%, from Sigma-Aldrich, were utilized for covalently coupling chitosan to corona-functionalized PE surface. N,N′-Carbonyldiimidazole (CDI) reagent (Sigma-Aldrich) is a highly active carbonylating agent that contains two acylimidazole leaving groups. CDI was used to activate carboxylic or hydroxyl groups for conjugation with other nucleophiles, creating either zero-length amide bonds or one-carbon-length N-alkyl carbamate linkages between cross-linked molecules.[22]

Surface Modification of PE

The procedure for surface modification of the inert PE surface was described in a previous paper.[16] Briefly, PE was corona treated in order to incorporate mainly new oxygen containing functional groups (PEc), improving the adhesion with the bioactive compound. Chitosan coating on the PE surface was achieved by dipping the PEc films into 1 wt % chitosan solution. The chitosan solution was prepared in twice-distilled water containing 8% acetic acid and 30% ethanol to facilitate film formation and subsequent solvent evaporation. Chitosan was immobilized on the PEc film surface by means of coupling agents (EDC/NHS and CDI).

The solution of 75 m*M* EDC + 15 m*M* NHS in water was used to activate the carboxylic groups formed at the PE surface after corona pretreatment. The CDI solution (20 m*M* concentration) prepared in ethanol, with a water content smaller than 0.1%, could activate both carboxyl and hydroxyl groups formed at the PE surface after corona pretreatment. The chitosan-coated films were washed with double-distilled water and dried, first at room temperature and subsequently in vacuum, at 50°C for 24 h.

The samples studied are the native PE, the corona-treated PE (PEc) and coated with chitosan by physical adsorption (PE/CHT) or by grafting using the two different coupling systems,

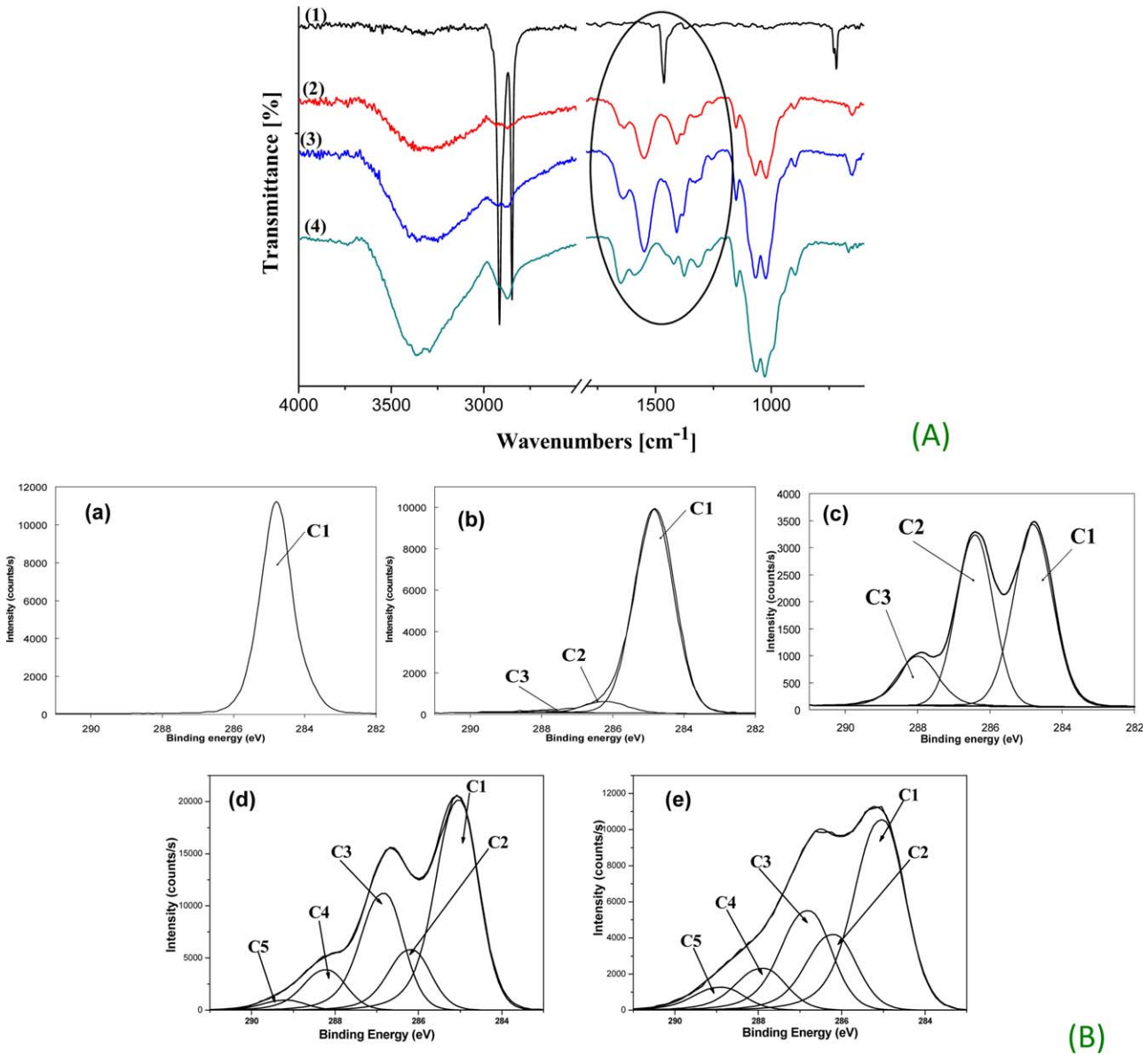

Figure 1. (A) ATR-FTIR spectra of chitosan-coated PE substrate: (1) PE; (2) PEcor/EDC+NHS/CHT; (3) PEcor/CDI/CHT; and (4) CHT; (B) XPS C1s core level spectra deconvolution of chitosan-modified PE substrate: (a) PE; (b) PEcor; (c) PEcor/CHT; (d) PEcor/EDC+NHS/CHT; (e) PEcor/CDI/CHT. C1, C2, C3, C4, and C5 denote the type of the carbon which is involved in different bonds, namely: C1—C-C, C-H, C2—C-NH_2 and/or C-O-C, C3—C-O, C4—N-C=O, and C5—O=C-O, respectively. [Color figure can be viewed in the online issue, which is available at wileyonlinelibrary.com.]

which are named here as (PEc/EDC+NHS/CHT) and (PEc/CDI/CHT), respectively.

Corona discharge treatment of the PE leads to the implantation of oxygen containing groups onto the surface[12] which react with chitosan amino groups, forming stable amide bonds or N-alkyl carbamate linkage depending on the coupling agent used, as revealed by ATR-FTIR spectroscopy measurements. In our previous paper[16] is presented the mechanism of PE surface functionalization and chitosan grafting in detail. Moreover, the stability of grafted chitosan layer on PE in harsh acidic medium has been proven.

Covalent bonding of chitosan was proved by ATR-FT-IR spectroscopy (spectra being recorded with a Bruker VERTEX 70 spectrometer, in the 600 to 4000 cm^{-1} wave number range and collected as 64 co-added scans at 2 cm^{-1} resolution). In the ATR-FTIR spectrum (see Figure 1A) of chitosan-coated PE the characteristic amine and Amide I bands appear at 1597 and 1651 cm^{-1}. After chemical coupling new absorption bands appear at lower wavenumbers, located at 1635 and 1548 cm^{-1}, when using EDC and NHS coupling agents and at 1639 and 1548 cm^{-1} in the case of CDI coupling route proving the formation of new bonds. These bands are assigned to stretching vibration of –C=O (Amide I), and to the δNH (in-plane deformation vibrations), respectively.

Were performed also X-ray photoelectron spectroscopy (XPS) measurements with a KRATOS Axis Nova, Kratos Analytical

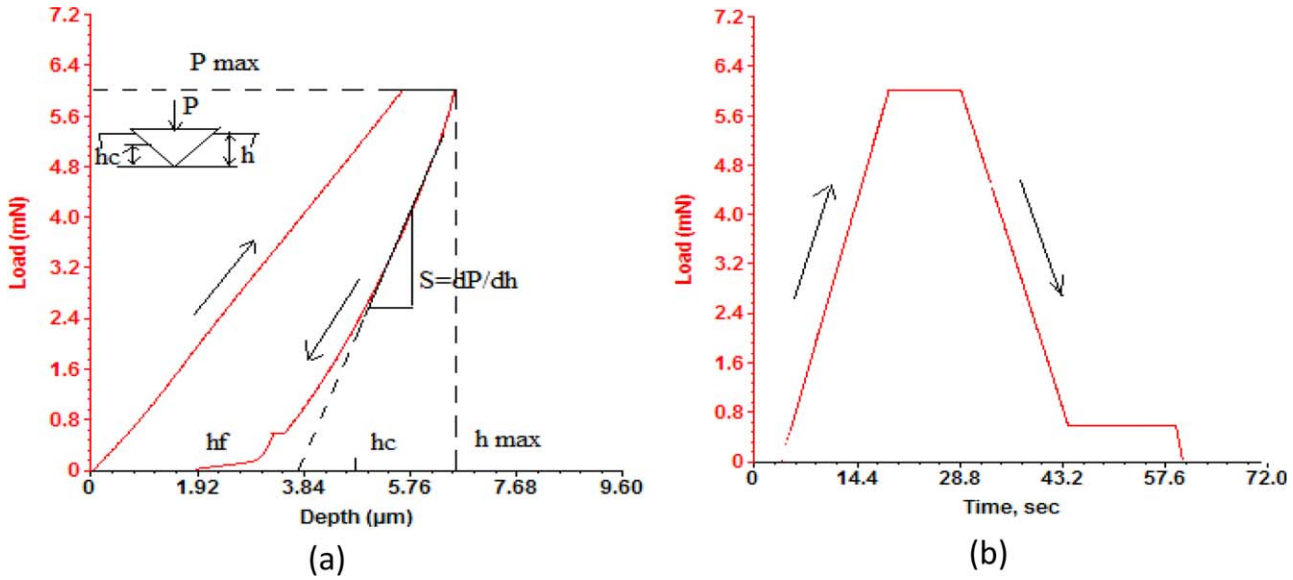

Figure 2. (a) Representative load–displacement curve and (b) load vs. time curve of one cycle indentation test. *P*—load; *h*—total depth of penetration; h_c—contact depth; h_f—depth of imprint after unloading. Arrows show the load and upload steps. [Color figure can be viewed in the online issue, which is available at wileyonlinelibrary.com.]

instrument (Manchester, United Kingdom) using AlKα radiation, with 20 mA current and 15 kV voltage (300 W), and base pressure of 10^{-8} to 10^{-9} Torr in the sample chamber. High resolution C1s spectra give information regarding the chemical composition of the surface. C1s high-resolution spectrum of PE presents one peak (C1) assigned to C-C and/or C-H, while C1s spectra of the plasma-treated and chitosan-modified samples were curve-fitted with three or five peak components from chemically nonequivalent carbon atoms mainly bonded to oxygen, in the case of corona discharge activated sample, and to nitrogen for samples coated with chitosan—Figure 1(B). Using the coupling agents two additional peaks are evidenced in the C1s spectra at 288 eV (C with O, C=O group and amide bond) (C4) and 289 eV (ester group) (C5). The C4/C2 atomic ratio of all chitosan coated sample increases after using both coupling routes, from 0.3 in the case of PEcor/CHT sample to 0.55 and 0.6 in the case of using CDI and EDC+NHS coupling agents, respectively, indicating the covalent bonding of chitosan onto plasma-treated PE surface.

Investigation Methods

Nano-Indentation. Nanomechanical fine analyses are performed at OLEM (IMech-BAS) using Universal Nanomechanical Tester (UNMT), produced by Bruker Surface Analysis, USA. It consisted of three analytical tools: a nano-indenter (Nanohead with optical microscope and CCD camera), Atomic Force Microscope (QScopeTM 250/400), and profilometer (PRO500 3D). This complex equipment allows performing a multi-field investigation on surface morphology. No surface smoothing was needed for the samples designed for the nano-indentation. All samples were cut to the proper dimensions (approximately to 0.25 cm^2, rectangular in the shape). Cut piece was then stuck to the metal cylinder with double sided adhesive tape, gently squeezed (the surface under investigation has to be flat) and then placed in the apparatus assembly. The sample surface was treated with the flush of canned air. Nano-indentations with the Nanohead module were conducted in order to calculate the hardness, Young's modulus of elasticity and contact stiffness.

The apparatus allows measurements to be carried out in three force channels from 1 to 150 mN. The test may be executed in two ways: single and multiple nano-indentations modes. For the purposes of the experiment, the multiple nano-indentation modes were chosen, this allowing us to study the mechanical properties variation with the load depth. The prepared software program (script) for this experiment consists of eight lines with 12 indentations each and spacing of 80 μm, covering a range of about 1 cm^2 on the surface. Each subsequent indentation from one line is with increasing force in the range from 2 to 6 mN. Between these values, 12 measuring points were specified, having maximum load of 2; 2.3; 2.7; 3; 3.3; 3.7; 4; 4.5; 5; 5.3; 5.7; and 6 mN. For each maximum load, the experiments were performed at three different locations on the test sample, covering various regions of the sample surface. Every single indentation experiment from this set consists of the following subsequent steps: (i) approaching the surface; (ii) loading to the peak load for 15 s; (iii) holding the indenter at peak load for 10 s; (iv) unloading from maximum force to 10% for 15 s; (v) holding at 10% of max force 15 s; (vi) final complete unloading for 1 s (load function 15–10—15 s trapezoid). The typical load–displacement and load–time dependencies of a viscoelastic material are shown in Figure 2(a,b).[23,24]

To correct for thermal drift, the nano-indentation instruments allow for a hold series of data points to be accumulated at either maximum load or at the end of the unloading from maximum load.[25] The first is creep within the specimen material as a result of plastic flow, which manifests itself when the load is held constant, and the depth readings increase as the indenter sinks into the specimen. In our test, the first hold step (iii) was included to avoid the influence of the creep on the unloading

characteristics of a viscoelastic material since the unloading curve was used to obtain the elastic modulus of the material. The second hold step (v) was also included at the end of the unloading from maximum load. Additionally, we put in our experiment the total time from the start of the test to the beginning of the unloading to be of 25 s, which is in the range of the time calculated for the PE film, using an equation proposed by Feng and Ngan.[25,26] They found that if the total time from the start of the test to the beginning of the unloading (t_h) has values in the range of the calculated by eq. (1), then the thermal drift has minimum effect on the calculated values of the elastic modulus (from an analysis of the unloading curve) of the tested material:

$$t_h \approx \frac{S}{|\dot{P}|} h_c \tag{1}$$

where S is the contact stiffness and $\dot{P}$ is the unloading rate, h contact depth at the maximal loading.

To properly determine the initial contact point and the accurate contact area, the pull-in interaction was accounted for in our nano-indentation experiments, as pointed by Wang *et al.*[27] Every indentation is started with the step called "Rough Approach to the samples" (it moves the nanohead down until the contact with the specimen surface is reached for the time-<5 min.) and step called "Fine Approach" (<2 s) which. This initial contact depth is usually made to be as small as possible. After this initial penetration, the real indentation starts. The initial penetration depth is corrected automatically for all displacement measurements.

The tip used for the nano-indentation process was a Berkovich Diamond with Tip Radius 70 nm. Olive-Pharr model was used for the calculation of nanomechanical characteristics, such as hardness and Young's modulus of elasticity [eqs. (2) and (3)].[28]

Hardness, H, is defined as the mean contact pressure, calculated by dividing the indenter load, P, by the projected contact area, A, at that load:

$$H = \frac{P}{A} \tag{2}$$

The projected contact area is dependent on the geometry of the indenter and is obtained from the contact depth of the indent, h_c, calculated from the total penetration depth h, indenter load P, and contact area $S = dP/dh$ at the beginning of unloading (Figure 2). The elastic modulus for the test material, E, is then calculated using Poisson's ratio of the test material, v, the modulus of the indenter, E_i, Poisson's ratio of the indenter, v_i, and the reduced modulus E_r:

$$\frac{1}{E_r} = \frac{1-v^2}{E} + \frac{1-v_i^2}{E_i} \tag{3}$$

For a diamond-tipped indenter, $E_i = 1141$ GPa and $v_i = 0.07$ GPa, thus the second term of the equation become negligible. The afore-mentioned procedure measures hardness and modulus at the maximum penetration depth of a single load–unload indent cycle.

Micro-Scratch Experiments. Micromechanical investigations are made using Mechanical and Tribology Tester (UMT-2M), Bruker, CETR. In Figure 3 the configuration for scratch experiments is showed. There are two types of scratch experiments that have been carried out on the chitosan-coated PE thin films:

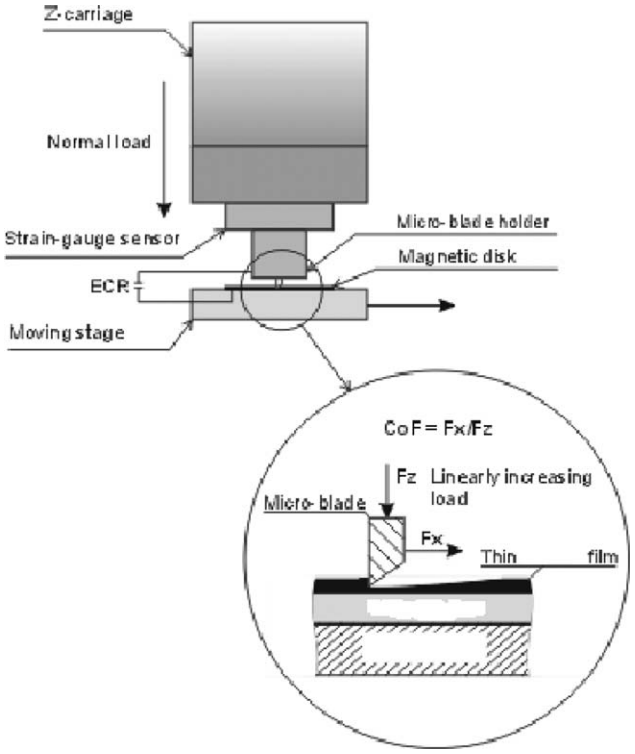

Figure 3. Scratch instrument configuration.

i. For constant force test the following experimental conditions have been used: Fz = 0.2 N = const; $\Delta X = 5$ mm; $V = 0.041$ mm/s. The normal force Fz exerts the predefined in the software constant load of 0.2 N during the entire scratch run of 5 mm displacement in X direction. The tangential force Fx is the one being observed throughout the experiment. The results are represented as graphs for the Scratch Coefficient of Friction (SCOF) and Z-displacement (depth of penetration). The Scratch Coefficient of Friction (SCOF) represents the ratio between the tangential and normal forces: COF = Fx/Fz

ii. The rising force test had the following experimental conditions: ΔFz = 2 N; $\Delta X = 5$ mm; $V = 0.041$ mm/s; usage of Electrical Current Resistance sensor (ECR). The normal force Fz exerts the predefined in the software interval load from 0 to 2 N during the entire scratch run of 5 mm displacement in X direction. Both the tangential force Fx and normal force Fz are being observed throughout the experiment. Here an Electric Current Resistance (ECR) sensor is also being utilized, in order to determine the exact point of tearing and the corresponding critical loads at which it occurs. For the purpose of this type of experiment the thin film sample is tightly fixated on a metal plate. With increasing the normal force the film tears at a point and this is registered by the ECR sensor. The ECR sensor response is observed when the scratching stylus comes into contact with the metal plate and electrical conductivity is recorded.

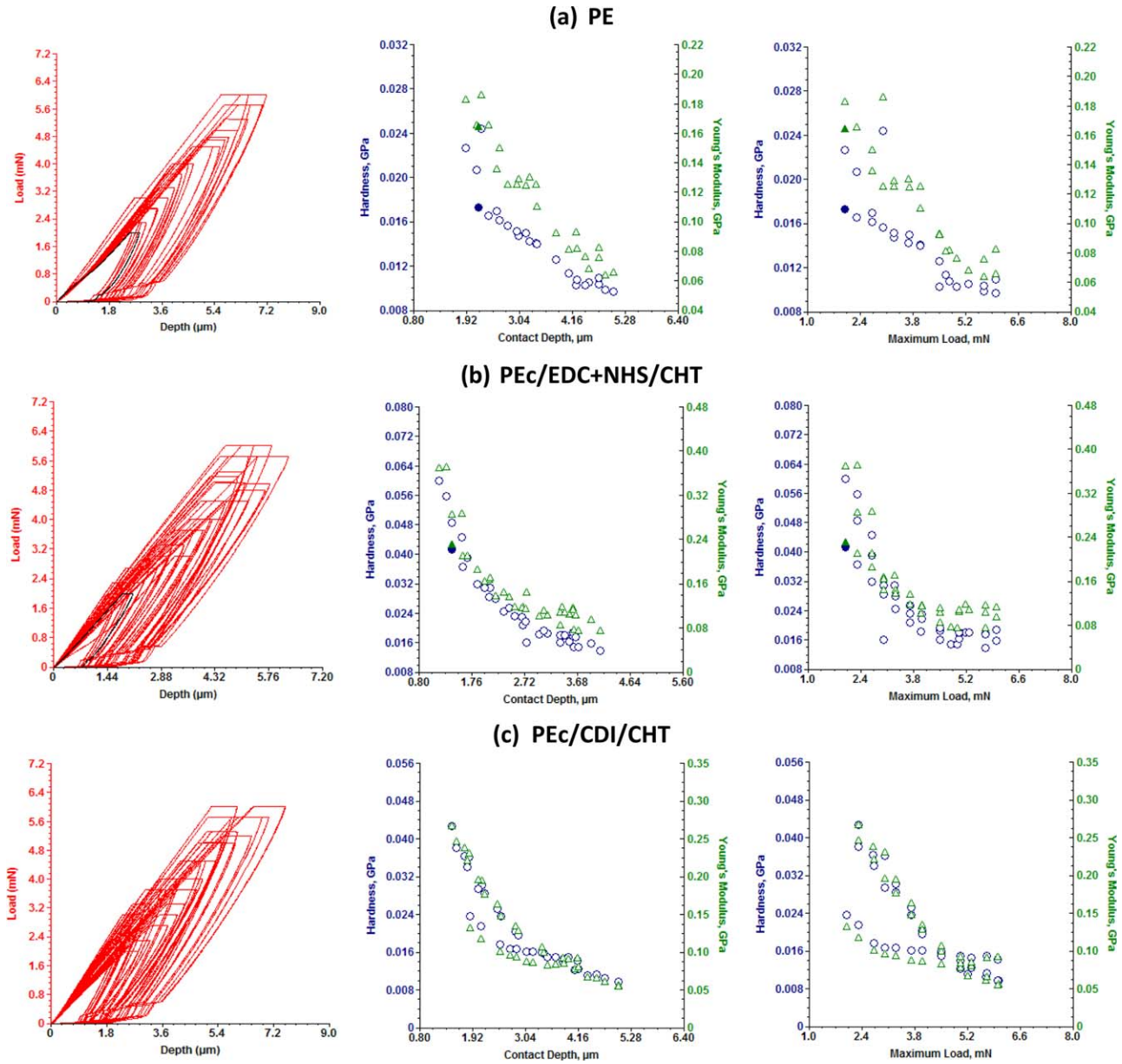

Figure 4. (a–c) Multicycle load–displacement curves with increasing force in the range of 2–6 mN and the calculated values of hardness and Young's modulus *versus* penetration depth and maximum load for the three tested samples: (a) PE; (b) PEc/CDI/CHT; (c) PEc/EDC+NHS/CHT. The experiments were performed at three different locations for each maximum load. [Color figure can be viewed in the online issue, which is available at wileyonlinelibrary.com.]

Oxygen Permeability Tests. Permeability tests were performed with a PERME™ OX2/231 Permeability Tester from Labthink Instruments, (Jinan, China) using oxygen as test gas (RH ~ 50%), at temperature of 23°C. Nitrogen was used as oxygen carrier. The oxygen flow rate was fixed at 20 mL/min while that nitrogen was 10 mL/min flow rate.

RESULTS AND DISCUSIONS

Nano-Indentation

The effect of functionalization of the PE surface by direct and covalent-bonded chitosan coating on the nanoscale mechanical properties of PE is studied by nano-indentation technique. Figures 4(a–c) present the multicycle load–displacement curves with increasing force in the range of 2–6 mN, as well as calculated values of hardness and Young' modulus vs. both the contact depth and the maximum load for the chitosan-grafted PE surfaces.

For every measured material a decrease of Young's modulus and hardness with increasing the applied force is observed. The contact depth for all the samples increases with the force applied to the tip, but keeps the values within the range of 1.5–5 μm (being smaller than the thickness of the chitosan layer which is 10 μm). Importantly, the contact depth at each load shows lower values for the chitosan-grafted PE films compared to the

Table I. Hardness Values of the investigated Samples at 12 Measuring Points of the Maximum Load in the Range 2–6 mN

	Hardness (MPa) at different forces (mN)												
Sample	2	2.3	2.7	3	3.3	3.7	4	4.5	5	5.3	5.7	6	Mean
PE	20.0	18.7	16.5	20.0	14.9	14.6	14.1	11.5	10.3	10.6	10.1	10.3	14.3 ± 5.7
PEc/EDC+ NHS/CHT	50.7	46.8	38.5	25.1	27.7	23.2	21.0	18.0	16.4	18.2	16.4	17.4	26.6 ± 11.4
PEc/CDI/CHT	23.6	34.1	29.4	27.5	25.1	21.6	18.6	15.6	13.7	12.7	12.2	11.2	20.4 ± 3.2

nonfunctionalized PE film, this confirming the improved mechanical properties of the PE surface by chitosan coating.

Tables I and II summarize the mean values of the mechanical characteristics Hardness and Young's modulus, respectively, at the 12 maximum loads (2; 2.3; 2.7; 3; 3.3; 3.7; 4; 4.5; 5; 5.3; 5.7; and 6 mN).

It is evident that an increase in both hardness and Young modulus occurred for the chitosan-coated PE samples compared with the substrate (neat PE). Chitosan grafting onto corona-treated PE surface using EDC/NHS coupling system leads to obtaining a harder surface than those using CDI one. If referred to the mean values, the hardness shows about 43% increase of its PE value in the case of PEc/CDI/CHT sample, whereas for PEc/EDC+NHS/CHT sample the increase has been even greater, subsequent 86%. Also Young's modulus follows the same change trend as the hardness does. However, this effect is strongly dependent on the applied maximum load value, which is expressed by the standard deviation. Importantly, the standard deviation of the PEc/EDC+NHS/CHT sample is much larger than those of the other test samples, PE and PEc/CDI/CHT. This result accounts for an inhomogeneous compactness of the structure in depth of the chitosan EDC/NHS/CHT coating, being very hard on the surface.

The sample obtained by physical adsorption of chitosan (PEc/CHT) onto corona-treated PE could not been analyzed by nano-indentation because the surface was too rough and this method is limited to smoother surfaces.

Atomic Force Microscopy results

Various ranges of the surface have been scanned namely beginning from 80 × 80 μm^2 until 1 × 1 μm^2 for each sample. Images have been recorded on different zones in order to be representative for the total sample surface state. Roughness of the neat PE and chitosan-coated surfaces was verified by statistical AFM estimations. The average vertical roughness (Ra) and horizontal roughness (Sm) has been calculated after a second-order flatness treatment of the raw data. The roughness values are based on standardized one-dimensional roughness parameters evaluation technique. Ra is the arithmetical average height of surface component (profile) irregularities from the mean line within the measuring length used to describe the vertical dimension of roughness. Sm is the mean spacing between peaks known as roughness spacing parameter that is used to describe the horizontal dimension of roughness.[29]

In Figure 5 are presented the AFM 2D images recorded for native and chitosan-grafted PE surfaces. The surface topography of PE changes after the chitosan covalent immobilization and new surface features are revealed.

It is evident that the chitosan-coated PE surfaces are much more homogeneous than the reference PE as the AFM roughness (listed in Table III). The PE surface grafted with chitosan by using EDC and NHS coupling agents system has a higher vertical roughness (Ra) compared with the sample grafted using CDI, but the lowest values of the horizontal roughness (Sm). Even if in depth irregularities for the PEc/EDC+NHS/CHT sample are more pronounced the mean spacing between peaks is narrower, which may indicate a more compact total surface area of this sample. The sample surface compactness is important for the surface mechanical properties of the coating, thus it will be further on correlated with micro-scratch characteristics.

Micro-Scratch Evaluation

Constant Normal Load Test. The results for the Scratch Coefficient of Friction (SCOF) and Z-displacement (depth of penetration) are obtained from the test. The value of the SCOF is defined as the ratio of the tangential force to the normal force—SCOF = Fx/Fz. The SCOF depends on several factors including the indenter geometry, surface roughness and the material properties. Rather than just being a friction parameter this value is a measure of the resistance to scratch depending

Table II. Young's Modulus of the investigated Samples at 12 Measuring Points of the Maximum Load in the Range 2–6 mN

	Young's modulus (MPa) at different forces (mN)												
Sample	2	2.3	2.7	3	3.3	3.7	4	4.5	5	5.3	5.7	6	Mean
PE	174	166	143	156	127	127	118	93	76	68	70	74	116 ± 58
PEc/EDC+ NHS/CHT	301	289	228	159	151	124	110	100	97	113	98	104	156±145
PEc/CDI/CHT	132	210	186	174	154	132	117	96	85	78	73	68	125 ± 57

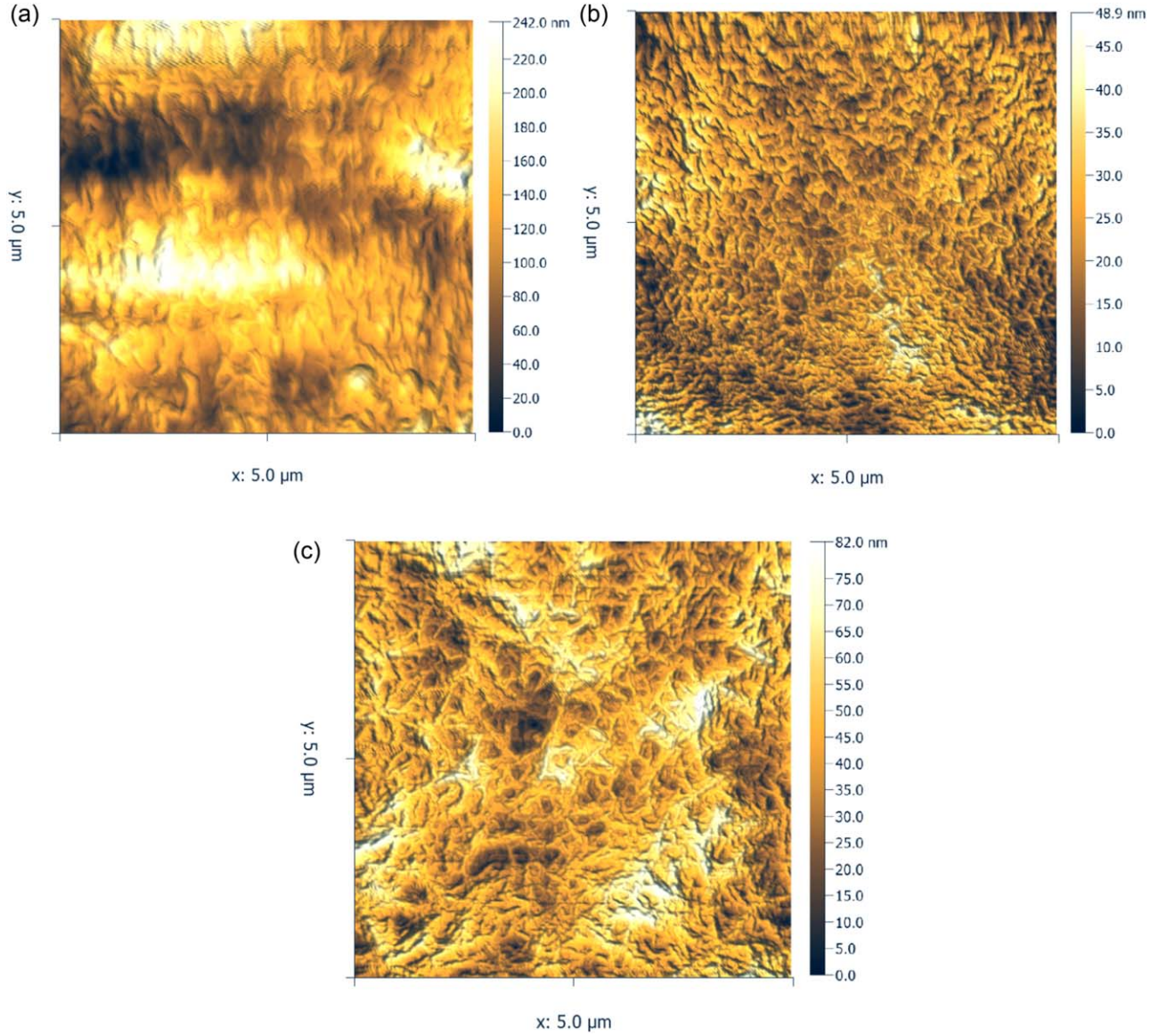

Figure 5. AFM 2D micrographs for: (a) reference PE; (b) PEc/EDC+NHS/CHT; (c) PEc/CDI/CHT. [Color figure can be viewed in the online issue, which is available at wileyonlinelibrary.com.]

on the surface roughness. A smoother material surface would impose higher resistance to scratch. This effect is observed when comparing the results for surface roughness (Table III) with the results for SCOF and Z displacement in Table IV.

As shown in Table IV, the SCOF values of the chitosan-coated samples show clear tendency for a sharp decrease, as compared to the neat PE substrate. This effect is strongly dependent on the type of coating treatment. Thus, the corona-treated PE and coated with chitosan directly (PE/CHT) show slightly lower values of SCOF, compared to the neat PE. In contrast, the chitosan-coated PE by using coupling agent systems demonstrate about 72% and 57% decrease of the SCOF values of the PEc/EDC+NHS/CHT and the PEc/CDI/CHT, respectively, compared to the reference neat PE, as well as to the PE/CHT film directly grafted chitosan film. The highly improved surface friction of the PE surface by such a chitosan coating is of significant importance for the interaction of the modified surfaces with cells developed in our further study.

If consider the Z-displacement values in Table IV, two orders of magnitude higher Z values appear for the chitosan-coated PE, as compared to the neat PE, because of the low resistance to scratch of the upper chitosan layer. However, compared to the directly coated chitosan (PE/CHT), the coated samples by using

Table III. The Calculated Roughness of the Investigated Samples at a 5 × 5 μm^2 Scanned Area

Samples	Ra (nm)	Sm (nm)
PE	33.8	34.6
PEc/EDC+NHS/CHT	19.3	5.4
PEc/CDI/CHT	10.3	7.8

Table IV. Micro-Scratch Mechanical Characteristics, SCOF and Z-Depth of Penetration

Samples	PE	PEc/CHT	PEc/EDC+NHS/CHT	PEc/CDI/CHT
SCOF (mean value)	2.335 ± 0.757	2.121 ± 0.918	0.661 ± 0.153	0.999 ± 0.193
Z- depth of penetration (mm)	0.00102±0.00896	0.11893 ± 0.01076	0.07772±0.00913	0.0450±0.00762

coupling agent systems EDC/NHS and CDI show much better resistance to scratch because of the improved compaction.

Micro-Scratch Tests with Increasing Normal and Tangential Loads. The obtained results from these experiments show the critical normal and tangential loads at which tearing of the whole system of substrate and coating occurs, these representing the tear resistance of the material in both directions. Figure 6 plots the tangential force (Fx) and normal force (Fz) values determined for native and chitosan-modified sample during the micro-scratch rising force test. As seen, the chitosan coating generally improves the tear resistance of the PE substrate, which is more pronounced in the tangential (Fx) direction then in the normal one (Fz). The simple physical adsorption of chitosan layers onto corona functionalized PE (PE/CHT) improves about 120% the overall tear resistance of the PE substrate. On the other hand the covalent immobilization of the chitosan onto PE leads to about 220–260% improvement of the tear resistance in tangential direction and 140–230 times improvement in normal direction, where the systems using EDC/NHS coupling agent show lower values than those of the systems using CDI. As a conclusion, the covalent-bonded chitosan on PE produces a stable coating, resulting in obtaining a stratified composite film with strong resistance to tearing.

Oxygen Permeability. In Table V are listed the oxygen transmission rate values recorded for neat PE and chitosan-modified ones. The oxygen permeability of PE decreases by surface chitosan immobilization, the sample grafted with chitosan using EDC/NHS coupling agents presenting the lowest value. On the basis of those presented above it can be stated that, the decrease of oxygen transmission rate is directly correlated with the surface compactness. As seen above, the PEc/EDC+NHS/CHT sample had the narrower spacing between mean peaks and therefore the lowest oxygen transmission rate.

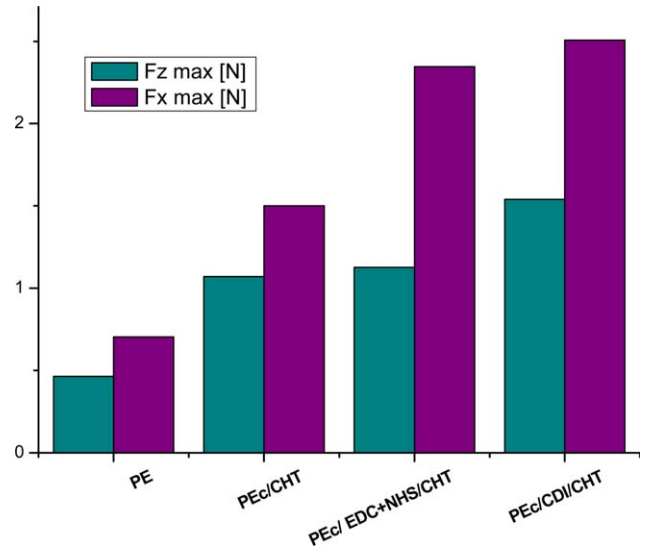

Figure 6. Tangential force (Fx) and normal force (Fz) determined for native and chitosan-modified sample during the micro-scratch rising force test. [Color figure can be viewed in the online issue, which is available at wileyonlinelibrary.com.]

The thickness of all studied samples was approximately constant to 10 μm and applied nano-identation method measures only at a certain depth of the surface layer (Table V). Therefore the dependence of surface mechanical properties on thickness of coating was not established. However, other properties depend on coating thickness as it was found by examination of properties determined in previous paper[2,16] and the results obtained here.

The film thickness of chitosan was determined by examination of the cross section, through fracture analysis, by scanning electron microscopy (SEM). Some of the investigated properties, like elemental composition, surface charge, oxygen permeability, and antimicrobial activity depend on the thickness of the deposited chitosan coating—Table VI.

Morphology of the surface also influences these properties, therefore the dependence is complex.

CONCLUSIONS

The effect of functionalization of the PE surface by physical adsorption and covalently bonded chitosan coating on the mechanical properties of PE was studied. The ability of nano-indentation and micro-scratch testing was explored to determine surface mechanical properties of chitosan-coated PE films. It has been established that the surface mechanical properties of PE film were improved by coating with grafted chitosan.

The results show that the chitosan grafting onto corona functionalized PE surface using various chemical agents strongly improve the surface hardness Young's modulus, and friction behavior, the best results being obtained by using EDC/NHS

Table V. Oxygen Permeability for Chitosan-Coated PE Films

Samples	Oxygen transmission rate (mL/m^2*day)
PE	3833.5
PEc	4226.8
PEc/CHT	2150.1
PEc/CDI/CHT	1765.4
PEc/EDC+NHS/CHT	1435.8

Table VI. Dependence of Various Properties of Chitosan-Coated PE on the Deposited Layer Thickness

	Property		
Thickness of surface layer	Surface charge (mmol/kg)	*Escherichia coli* inhibition activity, at 48 h (%)	Oxygen transmission rate (OTR) (mL/m^2*day)
10–50 μm	536.21	51	2150
8–15 nm	78.02	79	2952

coupling agent system. The surface mechanical properties influence the oxygen transmission rate of PE, higher the compactness smaller the oxygen permeability.

Compared to the neat PE substrate, the chitosan-coated samples using coupling agent systems show strongly improved tear resistance, where the coatings using CDI system show slightly better tear resistant performance than those using EDC/NHS. The surface roughness features are proportionally correlated with the micro-mechanical parameters, namely the surface is stiffer as the more compact it is. The improved surface mechanical properties and oxygen barrier of the chitosan-coated PE film by using EDC/NHS and CDI coupling agent systems demonstrate that it is possible to control the interactions of the modified surfaces with cells and to protect the food products.

The surface modified PE seems to be a promising material for biomedical/food packaging applications because of the well-known biocompatibility, low immunogenicity, and antimicrobial activity of the chitosan attached to the surface.

ACKNOWLEDGMENTS

The authors acknowledge the financial support given by the European Cooperation in Science and Technology (COST) action FA0904 (Eco-Sustainable Food Packaging Based on Polymer Nanomaterials); MP1202 (Rational design of hybrid organic-inorganic interfaces); bilateral project DNTC/India 01/10-2013 and IAEA Research Contract No: 17689 (RC-17689-R0).

REFERENCES

1. Chen, Y.; Liu, P. *J. Appl. Polym. Sci.* **2004**, *93*, 2014.
2. Munteanu, B. S.; Pâslaru, E.; Fras Zemljic, L.; Sdrobiş, A.; Pricope, G. M.; Vasile, C. *Cell. Chem. Technol.* **2014**, *48*, 565.
3. Bandopadhay, D.; Tarafdar, A.; Panda, A. B.; Pramanik, P. *J. Appl. Polym. Sci.* **2004**, *92*, 3046.
4. Tihminlioglu, F.; Dogan Atik, I.; Özen, B. *J. Food Eng.* **2010**, *96*, 342.
5. Mao, C.; Qiu, Y. Z.; Sang, H. B.; Mei, H.; Zhu, A. P.; Shen, J.; Lin, S. C. *Adv. Colloid Interface Sci.* **2004**, *110*, 5.
6. Sugiyama, K.; Matsumoto, T.; Yamazaki, Y. *Macromol. Mater. Eng.* **2000**, *282*, 5.
7. Lei, J. X.; Liao, X.; Gao, J. *Acta Chim. Sinica* **2001**, *59*, 685.
8. Hsiue, G. H.; Yang, J. M.; Wu, R. L.; *J. Biomed. Mater. Res.* **1988**, *22*, 405.
9. Mao, C.; Yuan, J.; Mei, H.; Zhu, A. P.; Shen, J.; Lin, S. *Mater. Sci. Eng. C* **2004**, *24*, 479.
10. Zhao, G. W.; Chen, Y. S.; Dong, T.; Xiaoli, W. *Plasma Sci. Technol.* **2007**, *9*, 202.
11. Shan, B.; Yan, H.; Shen, J.; Lin, S. C. *J. Appl. Polym. Sci.* **2006**, *101*, 3697.
12. Robertson, G. L. Food Packaging: Principles and Practice; Marcel Dekker: New York, **1993**.
13. Shin, G. H.; Lee, Y. H.; Lee, J. S.; Kim, Y. S.; Choi, W. S.; Park, H. J. *J. Agric. Food Chem.* **2002**, *50*, 4608.
14. Popelka, A.; Novák, I.; Lehocky, M.; Junkarc, I.; Mozetič, M.; Kleinová, A.; Janigová., I.; Slouf, M.; Bílek, F.; Chodák, I. *Carbohydr. Polym.* **2012**, *90*, 1501.
15. Theapsak, S.; Watthanaphanit, A.; Rujiravanit, R. *ACS Appl. Mater. Interfaces* **2012**, *4*, 2474.
16. Paslaru, E.; Fras Zemljic, L.; Bracic, M.; Vesel, A.; Petrinic, I.; Vasile, C. *J. Appl. Polym. Sci.* **2013**, *130*, 2444.
17. Moghbeli, M. R.; Mohammadi, N.; Zanjirian, E. in Advances in the Bonding of Rubber to Various Substrates, Proceedings of Rubber Bonding Conference, Cologne, Germany, Nov 20–21, 2001.
18. Ho, E.; Marcolongo, M. *Dent. Mater.* **2005**, *21*, 656.
19. Amendola, E.; Cammarano, A.; Acierno, D. A Study of Adhesion of Silicon Dioxide on Polymeric Substrates for Optoelectronic Applications, Optoelectronic Devices and Properties, www.intechopen.com (accessed January 25, **2015**).
20. Odegard, G. M.; Gates, T. S.; Herring, H. M. *Soc. Exp. Mech.* **2005**, *45*, 130.
21. Broughton, W. R.; Crocker, L. E.; Loderio, M. J. NPL Report DEPC-MPR 055. http://www.npl.co.uk/publications/characterising-micro-and-nanoscale-interfaces-in-advanced-composites-a-review (accessed December 1, **2014**).
22. Anderson, G. W.; Paul, R. *J. Am. Chem. Soc.* **1958**, *80*, 4423.
23. Geng, K.; Yang, F.; Druffel, T.; Grulke, E. A. *Polymer* **2007**, *48*, 841.
24. Ivanov, E.; Borovanska, I.; Milosheva, B.; Kotsilkova, R. Experimental Nano and Micro Mechanics of Nanostructured Materials. In: Mechanics of Nanomaterials and Nanotechnology; Kavardjikov, V.; Parashkevova, L.; Baltov, A., Eds.; Science Series, Bulgarian Academy of Sciences, **2012;** pp. 287-326.
25. Fischer-Cripps, A. C. Nanoindentation, Mechanical Engineering Series; Springer: Berlin, **2011**, p 77.
26. Feng, G.; Ngan, A. H. W. *J. Mater. Res.* **2002**, *17*, 660.
27. Wang, Z.; Volinsky, A. A.; Gallant, N. D. *J. Appl. Polym. Sci.* **2014**, 131.
28. Oliver, W. C.; Pharr, G. M. *J. Mater. Res.* **1992**, *7*, 1564.
29. Marghalani, H. Y. *J. Appl. Oral Sci.* **2010**, *18*, 59.